ELSEVIER

Biochemical Pharmacology 62 (2001) 1337–1343

Biochemical Pharmacology

Impact of the basic amine on the biological activity and intracellular distribution of an aza-anthrapyrazole: BBR 3422

Kai-Ming Chou*,[1], A. Paul Krapcho[2], Miles P. Hacker[3]

Department of Pharmacology, University of Vermont School of Medicine, Burlington, VT 05405, USA

Received 17 January 2001; accepted 30 April 2001

Abstract

The anthrapyrazoles have entered clinical trials and show significant activity against breast cancer. However, these drugs are cardiotoxic and ineffective in multidrug-resistant (MDR) tumor cells. We have reported previously on the synthesis and antitumor characteristics of the 9-aza-anthrapyrazoles and their lack of cardiotoxicity; unfortunately, the leading candidates are cross-resistant in MDR-expressing cells. The results also indicated that the side arm structures of 9-aza-anthrapyrazole play a critical role in determining the drug resistance in MDR-expressing cells—only compounds that have a tertiary amine on both side arms are not cross-resistant. To further elucidate the biochemical and pharmacological impact of the side arm structures, one of the 9-aza-anthrapyrazole compounds, BBR 3422 {2-(2-aminoethyl)-5-(2-methylaminoethyl)indazolo[4,3-*g*,*h*]isoquinoline-6(2*H*)-one}, was selected to be photolabeled with *N*-hydroxysuccinimidyl-4-azidosalicylic acid (NHS-ASA). In comparison to the parental compound, the photolabeled BBR 3422 was not as cytotoxic or DNA active, but it competed better than the parental compound against azidopine on P-glycoprotein labeling. In addition, confocal microscopic studies showed that BBR 3422 was clustered mainly in the cell nucleus, but its photolabeled analogue was located in the cytoplasm of the human breast cancer cell line MCF-7. Only a trace amount of both compounds was detected in the doxorubicin-derived resistant cell line MCF-7/ADR. The treatment of MCF-7/ADR cells with verapamil increased the intracellular amounts of both compounds.

Keywords: Multidrug resistance; Aza-anthrapyrazole; P-glycoprotein; Intracellular distribution; DNA intercalation; Photoaffinity labeling

1. Introduction

Anthrapyrazoles, like CI-941, have entered clinical trials and have been shown to be effective against breast cancer [1,2]. However, like other clinically used anthracyclines or anthracenediones, cardiotoxicity and the lack of cytotoxicity against MDR-expressing cells remain to be the major drawbacks [3–8]. In an attempt to minimize the cardiotoxicity of these compounds, a new series of anticancer drugs—aza-anthrapyrazoles—was developed in our laboratory. As reported earlier [9], only the 9-aza-anthrapyrazoles have *in vivo* activity among other aza-anthrapyrazole compounds, which indicated that the nitrogen position on the C ring is critical in determining the efficacy of these compounds. With respect to MDR cross-resistance, the aza-anthrapyrazole compounds were cross-resistant when at least one side arm contained a terminal primary or a secondary amine; compounds having terminal tertiary amines on both side arms were not cross-resistant in MDR-expressing cells [9]. We have reported that the terminal primary amine side arms in anthracenediones and anthracyclines are critical for DNA binding affinity and drug potency [10,11].

Our previous data have shown that only the 9-aza compounds had significant *in vivo* antitumor activity among a series of aza-anthrapyrazoles in which the ring nitrogen was placed at different positions [9]. However, compounds having the greatest therapeutic activity were cross-resistant in MDR tumor cells [9]. MDR resistance can be caused by several mechanisms [12,13], and the overexpression of

* Corresponding author. Tel.: +1-203-785-7119; fax: +1-203-785-7129.

E-mail address: Kai-Ming.Chou@VTMEDNET.ORG (K-M. Chou).

[1]Present address: Department of Pharmacology, Yale University School of Medicine, 333 Cedar Street, SHM B-315, New Haven, CT 06520.

[2]Present address: Department of Chemistry, University of Vermont, Burlington, VT 05405.

[3]Present address: Department of Health Sciences, Grand Valley State University, Allendale, MI.

Abbreviations: MDR, multidrug resistance; NHS-ASA, *N*-hydroxysuccinimidyl-4-azidosalicylic acid; SRB, sulforhodomine B; and P-gp, P-glycoprotein.

0006-2952/01/$ – see front matter
PII: S0006-2952(01)00797-3

membrane-bound P-gp is one of the major mechanisms [14]. P-gp recognizes a broad variety of compounds and causes drug resistance by reducing the intracellular concentration of the compounds by pumping them out of the cell in an energy-dependent manner [15,16]. For both aza-anthracycline and aza-anthrapyrazole compounds, the side arm structure plays a critical role in determining the pharmacological and biochemical characteristics of a compound [9–11]. We reported that both series of compounds were active in MDR cells when both of the side arms had tertiary terminal amines but were cross-resistant if one of the side arms was a primary or secondary amine [9–11].

The photoaffinity labeling technique has been widely used to investigate the interaction between P-gp and various anticancer drugs. Since the structure of the side arms of aza-anthrapyrazole plays an important role in determining their activities in MDR-expressing cells, the photoaffinity labeling modification could also cause some changes in properties of the original compound. To further address the impact of the side arm structures on the biological and pharmacological activities of the 9-aza-anthrapyrazoles, the photoaffinity analogue of the aza-anthrapyrazole BBR 3422 {2-(2-aminoethyl)-5-(2-methylaminoethyl)indazolo[4,3-*g*,*h*] isoquinoline-6(2*H*)-one} was synthesized by coupling with NHS-ASA through the primary amine side arm (Fig. 1).

The cytotoxicity and DNA intercalation ability of the photolabeled analogue of BBR 3422, as well as its binding affinity toward P-gp, were studied in this report. Since the intracellular distribution patterns of anthracyclines have been shown to be different between sensitive and resistant tumor cell lines [17], we hypothesized that this phenomenon could be critical for the toxicity of the drugs. Our laboratory previously reported that anthracyclines having primary or secondary amine side arms were clustered in the cell nucleus, whereas compounds having tertiary amines on both side arms localized in distinct cytoplasmic vesicles [18]. Therefore, the influence of the photoaffinity labeling of BBR 3422 on its intracellular distribution was also addressed in this report.

2. Materials and methods

2.1. Drugs

[^{3}H]Azidopine was purchased from Amersham. BBR 3422 was synthesized by Boehringer Mannheim. The purity of this compound was determined by HPLC, NMR, TLC, and elemental analysis. To obtain free base BBR 3422, BBR 3422 was dissolved in H_2O and mixed with an equal volume of 0.2 M $Na_2B_4O_7$; the free base drug was then extracted repeatedly with chloroform. The purity of the free base drug was assured by NMR, TLC, and LC mass spectrometry.

a. BBR 3422

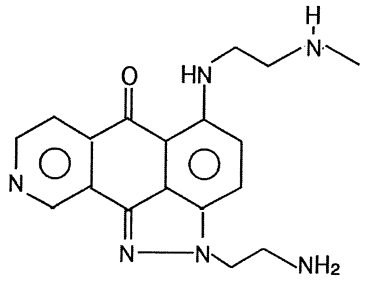

b. Photolabeled BBR 3422

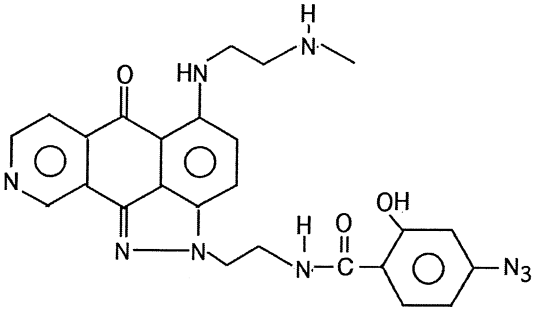

Fig. 1. Chemical structures of the compounds.

2.2. Photolabeling

The photoaffinity probe NHS-ASA was purchased from the Pierce Co. The free-base BBR 3422 was dissolved in DMSO to which NHS-ASA was added at a 1:1 molar ratio (NHS-ASA:drug) and incubated overnight at 4°. The product was analyzed by silica gel TLC with a solvent system containing 90 mL chloroform, 10 mL methanol, and 3 mL water. To purify the photolabeled BBR 3422, the reaction mixture was dried by speed vacuuming and redissolved in 50% acetonitrile for injection into an HPLC C18 column (Waters Co.). The product was eluted with a 50–100% acetonitrile gradient, and the purity was verified by NMR and LC mass spectrometry.

2.3. Cytotoxicity

Both the sensitive MCF-7 and the resistant MCF-7/ADR human breast cancer cell lines were grown in RPMI 1640 medium (Sigma) supplemented with 10% fetal bovine serum (HyClone), 1% glutamine (Gibco BRL), and 1% antibiotic/antimycotic (Gibco BRL), in a humidified atmosphere of 5% CO_2. An additional 0.5 μg/mL of doxorubicin was added to the MCF-7/ADR cell-maintaining medium.

Doxorubicin was removed from the medium 7–10 days before the cells were used for experiments. For cytotoxicity assays, exponentially growing cells were diluted in fresh medium to approximately 10,000 cells/mL. The cells were subsequently treated with different concentrations of drugs for 72 hr at 37° before the addition of 50 μL of 50% trichloroacetic acid (TCA) for another 2 hr at 4°. The medium was discarded, and SRB was added at room temperature over a 30-min period. The SRB was washed off with Tris–HCl (pH 7.5) buffer, and the plates were air-dried before the addition of H_2O to dissolve the dried SRB. The absorbance was read using a plate reader (Bio-Tek Instruments) set to a wavelength of 570 nm.

2.4. DNA unwinding assay

DNA unwinding caused by the drug was measured by monitoring electrophoretic mobility changes of supercoiled pBR322 DNA (U.S. Biochemicals) in 1.4% agarose gels (Gibco BRL) in the presence of different concentrations of drugs. The drugs were incubated with pBR322 DNA for 15 min in 250 mM NaCl, 25 mM HEPES, pH 7.5, and 1 mM EDTA before being subjected to gel electrophoresis. The electrophoretic buffer contained 89 mM Tris–HCl, pH 8.0, 89 mM boric acid, and 0.2 mM disodium EDTA. The gel was stained with 5 μg/mL of ethidium bromide after electrophoresis, and photographs of each gel were taken under UV light.

2.5. Cell membrane preparation

Cells from the exponentially growing MCF-7 cell line and the doxorubicin-resistant MCF-7/ADR cell line were harvested and resuspended in a hypotonic buffer [5 mM Tris, 2 mM EDTA, pH 7.4, 0.1 mM phenylmethylsulfonyl fluoride (PMSF)]. The cells were kept on ice for 30 min before being homogenized. The cell homogenate was spun at 1000 *g* for 10 min at 4°. The supernant was recentrifuged at 100,000 *g* for 1 hr at 4°. The membrane pellet was resuspended in a membrane storage buffer (10 mM Tris, 100 mM NaCl, 2 mM EDTA, 20% glycerol, 0.1 mM PMSF) at a protein concentration of 50 μg/mL and stored at −80°.

2.6. P-gp photolabeling

[^{3}H]Azidopine (1.25 μM) was incubated with 10 μg of membrane preparation and different concentrations of drugs for 20 min at 25°. Cross-linking reactions were carried out at 25° by exposing the reaction mixtures under a UV lamp (wavelength 263 nm) for 20 min. The reaction mixtures were applied onto an 8% SDS–PAGE gel for electrophoresis. The gel was dried on a gel dryer (Speed gel, SG210G, Savant) and then exposed to a chemoilluminant film (Amersham). The bands were quantified using a PDI Quantity 1 densitometer (model DNA 35, PDI, Inc.).

Table 1
Cytotoxicities of BBR 3422 and photolabeled BBR 3422

	Drug (μg/mL)	
	MCF-7	MCF-7/ADR
BBR 3422	0.09	0.7
Photolabeled BBR 3422	1.1	5.4

Dissolved drugs were added to the cell culture medium of MCF-7 and MCF-7/ADR cells. The cell numbers were counted after a 72-h incubation, and growth inhibition was calculated. The IC_{50} values were calculated as the drug concentration needed to inhibit cell growth by 50% in comparison with the untreated controls. The IC_{50} values were obtained from triplicate experiments, and the error range was less than 5%.

2.7. Confocal microscopy

Approximately 4×10^5 cells supplemented with growth medium (RPMI 1640) were grown overnight on a glass coverslip at 37°. BBR 3422 (1 μM) or photolabeled BBR 3422 (1 μM) was added to the cells for 30 min at 37°. For verapamil or methylamine treatment, the cells were incubated with verapamil (50 μM) with or without methylamine (5 mM) for 1 hr at 37° before the addition of the test compounds. The coverslips were rinsed with PBS before being mounted on slides and observed with an Olympus BX50 epi-fluorescence light microscope.

For the determination of the subcellular distribution of BBR 3422 and its photolabeled analogue, a Bio-Rad MRC-100 Laser Scanning Confocal Microscope mounted on an Olympus BX50 upright microscope equipped with a krypton/argon laser was utilized. The distribution was observed at an excitation wavelength of 488 nm with a laser setting at 30%, an iris of 3.2, and a gain setting at 1250 V. Relative cellular intensity was also determined from the drug distribution studies by keeping the laser, iris, and gain setting constant from sample to sample.

3. Results

3.1. Cytotoxicity

The cytotoxicities of BBR3422 and its photolabeled analogue were compared in both wild-type MCF-7 and the derivative MCF-7/ADR (MDR) resistant cell lines. As shown in Table 1, the photolabeled analogue was 12-fold less potent than the parental compound in MCF-7 cells and about 8-fold less potent in the MDR cells. These data suggested that basic amines on both side arms are necessary for the maximum cytotoxic effect of the drug.

3.2. DNA retardation gel assay

Previous data have shown that one of the major mechanisms of action of anthrapyrazoles is through DNA intercalation [19,20], which results in DNA torsion and conforma-

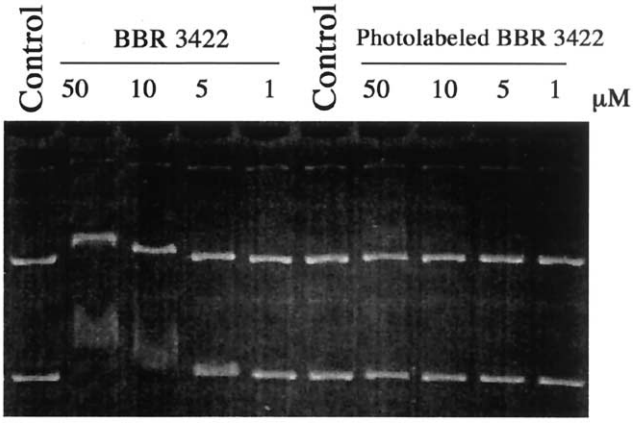

Fig. 2. DNA migration assay. Different concentrations of the test compounds were incubated with pBR322 DNA in 25 mM HEPES, pH 7.5, 500 mM NaCl, and 1 mM EDTA at 37° for 20 min before loading onto a 1.4% agarose gel for electrophoresis. The gel was stained with ethidium bromide, examined with UV light, and photographed.

tional changes, thereby blocking DNA replication. The intercalation of the drug into the DNA molecule causes DNA conformation changes and affects the electrophoretic mobility of DNA. As shown in Fig. 2, at a concentration of 5 μM, BBR 3422 altered DNA migration and slowed it dramatically at 10 μM. In contrast, up to a 50 μM concentration of the photolabeled analogue had no apparent affect on DNA migration. These results indicated that the photolabeled analogue was less cytotoxic and had lower affinity for DNA than did BBR 3422.

3.3. Competition against [^{3}H]azidopine in P-gp labeling

Since BBR 3422 is cross-resistant in MDR cells overexpressing P-gp, the P-gp binding affinities of BBR 3422 and its photolabeled analogue were compared by inhibiting [^{3}H]azidopine binding to P-gp (Fig. 3). Vinblastine, a known inhibitor of azidopine binding to P-gp [21], was used to confirm the labeling specificity and inhibited azidopine labeling at 125 μM (Fig. 3, lane 2) (Table 2). BBR 3422 was able to inhibit 25% of azidopine labeling when its concentration was 100-fold higher than that of azidopine;

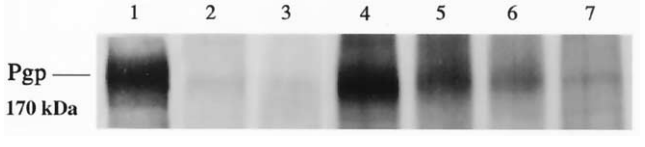

Fig. 3. Competition assay for P-gp binding. [^{3}H]Azidopine (1.25 μM) and different concentrations of compounds were incubated with 10 μg of MCF-7/ADR cell membrane preparations at room temperature for 20 min before exposing to UV light. The samples were loaded onto an 8% SDS–PAGE gel for electrophoresis. After electrophoresis, the gel was dried and exposed to a chemoilluminant film. The bands were quantified using a PDI quantity I densitometer. Lane 1: azidopine alone. Lane 2: vinblastine (125 μM). Lane 3: verapamil (125 μM). Lanes 4–6: BBR 3422 (125, 625, and 1250 μM, respectively). Lane 7: photolabeled BBR 3422 (125 μM).

Table 2
Percent inhibition of P-gp labeling

	% Inhibition
Vinblastine	89.8 ± 3.94
Verapamil	93.0 ± 1.91
BBR 3422 (125 μM)	20.2 ± 3.81
BBR 3422 (625 μM)	50.9 ± 5.56
BBR 3422 (1.25 mM)	70.7 ± 5.88
Photolabeled 3422 (125 μM)	84.0 ± 1.50

The methods for this experiment are as described in the legend of Fig. 3. The percent inhibition was calculated by dividing the intensity of the P-gp band by the total intensity of the whole lane. The percentages of inhibition of different compounds were adjusted using the azidopine-labeled P-gp as a 100% standard. The values presented in the table are means ± range of two independent experiments.

71% inhibition was observed at a concentration of 1.25 mM (Table 2). Surprisingly, the photolabeled analogue of BBR 3422 inhibited azidopine labeling more effectively than did the parent compound. At 100-fold molar excess (125 μM), the photolabeled compound inhibited azidopine binding by 84%, suggesting it has a higher affinity for P-gp than BBR 3422.

3.4. Intracellular drug distribution

Since the aza-anthrapyrazoles are intensely fluorescent, we were able to investigate the intracellular distribution of these compounds using laser confocal microscopy. Our laboratory has observed that all the aza-anthrapyrazole compounds, which have at least one side arm with a terminal primary or secondary amine, were cross-resistant in MDR cells and concentrated in the cell nucleus of MCF-7 cells [18]. In contrast, if the compound bore a tertiary amine on both side arms, it was not cross-resistant and was located in the cytoplasm in a punctate pattern [18].

In accordance with previous results [18], BBR 3422 was clustered in the cell nucleus (Fig. 4a). In contrast, its photolabeled analogue, even with a free secondary amine side arm, was located in the cytoplasm instead of the cell nucleus (Fig. 4b).

As shown in panels c and d of Fig. 4, the MCF-7/ADR cells effectively pumped out both BBR 3422 and its photolabeled analogue, as little intracellular fluorescence could be detected. However, verapamil, a calcium channel blocker that has been used to reverse drug resistance in MDR-expressing cells [21,22], increased the intracellular fluorescence intensities of both compounds in the MCF-7/ADR cells. The parent BBR 3422 was also located in the cell nucleus in the verapamil-treated resistant cells. In comparison to BBR 3422, the photolabeled analogue was distributed in the cytoplasm in these verapamil-treated resistant cells.

It has been reported that doxorubicin is located in the nucleus of the sensitive MCF-7 cells but in the cytoplasmic acidic organelles (i.e. Golgi, endosomes, and lysosomes) of ADR-resistant cells [23]. To further address the subcellular

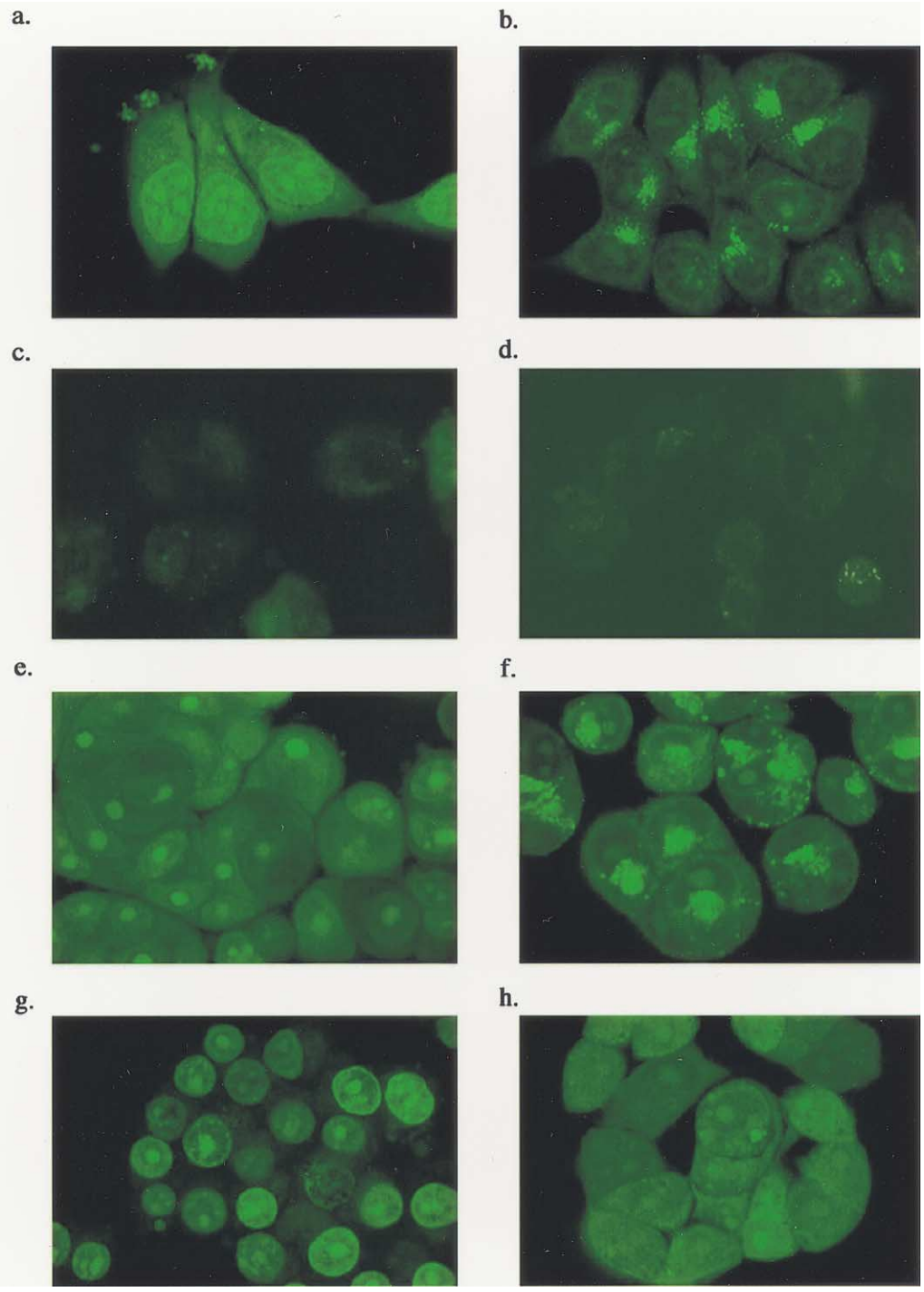

Fig. 4. Intracellular distribution of BBR 3422 and its photolabeled analogue. Cells were seeded and grown exponentially on coverslips overnight before a 1-hr treatment with different compounds. The coverslips were rinsed with PBS and mounted on slides for observation, using confocal microscopy. (a) BBR 3422 in MCF-7 cells. (b) Photolabeled BBR 3422 in MCF-7 cells. (c) BBR 3422 in MCF-7/ADR cells. (d) Photolabeled BBR 3422 in MCF-7/ADR cells. (e) BBR 3422 in verapamil-pretreated MCF-7/ADR cells. (f) Photolabeled BBR 3422 in verapamil-pretreated MCF-7/ADR cells. (g) BBR 3422 in verapamil- and methylamine-pretreated MCF-7/ADR cells. (h) Photolabeled BBR 3422 in verapamil- and methylamine-pretreated MCF-7/ADR cells.

organelle locations for the photolabeled analogue, both the resistant and sensitive cells were treated with methylamine in the presence or absence of verapamil. Methylamine becomes a highly positively charged molecule in acidic organelles and, therefore, increases the pH in those organelles [24]. The pH increase prevents the accumulation of positively charged drug in these acidic organelles [23]. The treatment with methylamine did not change the intracellular

distribution pattern of the photolabeled analogue of BBR 3422 in the sensitive cells (data not shown). However, in resistant cells co-treated with verapamil and methylamine, the distribution pattern of the photolabeled analogue changed from one that was cytoplasmic to one that was increasingly nuclear and nucleolar.

4. Discussion

In this study, BBR 3422, one of the 9-aza-anthrapyrazole compounds with a primary and a secondary terminal amine side arm, was modified by coupling an NHS-ASA photoaffinity probe through its primary amine group on the side arm to study the biological and biochemical importance of the basic amine group to this compound.

The cytotoxicity results indicate that the photoaffinity labeling reduced the potency of BBR 3422 in the MCF-7-sensitive and the resistant MCF-7/ADR cell lines 8- to 12-fold. These results suggest that the positively charged amine on the side arm is important for cytotoxicity. One of the major mechanisms of action of the anthrapyrazoles is through DNA intercalation and the subsequent production of photoinduced single-strand DNA breaks [19]. Although the photolabeled analogue of BBR 3422 may interact with DNA through different mechanisms, the results indicated that the photolabeled analogue of BBR 3422 has a decreased ability to intercalate into DNA in comparison with the parent compound. It has been reported that anthracyclines stack into the DNA double-helix structure with the chromophore backbone, and this drug–DNA complex is stabilized by the charged amine on the side arm [25–27]. It is possible that the protonated primary amine on the side arm of BBR 3422 is important in stabilizing the DNA–drug complex through the interaction with the negatively charged phosphate groups on the DNA molecule. These results suggest that DNA binding may play a role in determining aza-anthrapyrazole cytotoxicity.

Most anthrapyrazole compounds are cross-resistant in multidrug-resistant cells overexpressing P-gp [28]. In the current resistance model, this protein can recognize a wide spectrum of drugs and extrude them in an ATP-dependent process [15,16]. In this study, we compared the inhibitory effects of BBR 3422 and its photoaffinity analogue on azidopine binding to P-gp. The photolabeled analogue was a better competitor than the parent compound against azidopine. Lipophilicity has been shown to be an important factor in determining binding affinity of anthracycline-like compounds to P-gp [29–31]. Our observations are consistent with this finding since the photolabeled analogue was more lipophilic than BBR 3422. The higher lipophilic photoaffinity analogues may have longer retention times on the cell membrane, which increases the opportunity to interact with the membrane-integrated P-gp. However, it is possible that the mechanisms of the photolabeled compound for inhibiting azidopine binding to P-gp are different from the mechanisms of BBR 3422, since the photolabeled analogue upon exposure to UV light can form a covalent bond with P-gp. The relationship between the drug structure, lipophilicity, and interaction with P-gp needs to be investigated further.

The intracellular distribution patterns of BBR 3422 and its photoaffinity analogue behaved very differently from each other in MCF-7 cells. The parent compound concentrated in the cell nucleus, whereas the photolabeled analogue was excluded from the nucleus but located in the cytoplasm. The reduced cytotoxicity of the photolabeled analogue could be due, in great part, to its intracellular distribution. Since BBR 3422 has a higher affinity for DNA than its photolabeled analogue, it is likely that BBR 3422 binds to DNA once it enters the nucleus. In contrast, the photolabeled analogue, having a low affinity for DNA, likely does not bind to DNA and consequently is not retained in the cell nucleus. The majority of this photolabeled analogue was distributed in the cytoplasm around the nucleus, where the Golgi apparatus, endoplastic reticulum, and lysosomes are located. It is possible that the weaker charged photolabeled analogue is trapped once it diffused into these acidic organelles [23].

Reduced amounts of both compounds were observed in MCF-7/ADR cells compared with the parental MCF-7 cells. Verapamil, an inhibitor of the P-gp pump [21,22], prevented efflux of either drug from the resistant cells and, therefore, increased the intracellular fluorescent intensity of both BBR 3422 and its photolabeled analogue. For intracellular distribution, the photolabeled compound was located in a punctate pattern in the cytoplasm around the cell nucleus in the verapamil-treated resistant cells, while BBR 3422 was located in the nucleus.

P-gp is also located on the membrane of the Golgi apparatus [32]. Our results (Table 2) suggested that the photolabeled analogue has higher P-gp binding affinity than BBR 3422. It is possible that the photolabeled analogue was recognized by the P-gp on the membrane of the Golgi apparatus and was pumped into the acidic organelle.

For the resistant cells pretreated with verapamil and methylamine, the photolabeled analogue was distributed more uniformly in the cytoplasm. In addition, more of the drug was detected in the nucleus and nucleoli. This phenomenon was not observed in the sensitive cells treated with methylamine. Altan *et al.* [23] indicated that the pH values are different in the subcellular organelles in MCF-7 and MCF-7/ADR cells. It is possible that methylamine may not have the same impact on the sensitive cells as in the resistant cells due to the different pH values of their subcellular organelles [23,33,34]. In addition, the trapped photolabeled analogue in the Golgi apparatus may be transported into the lysosome more rapidly in the resistant cells than in the sensitive cells as a result of more active intracellular trafficking [35,36].

Acknowledgments

We would like to thank Dr. Lori Hazlehurst for insightful discussions and Dr. James Bigelow for assistance with HPLC.

References

[1] Blanz J, Renner U, Schmeer K, Ehninger G, Zeller KP. Detection and identification of human urinary metabolites of biantrazole (CI-941). Drug Metab Dispos 1993;21:955–61.
[2] Hortobagyi GN. Overview of new treatments for breast cancer. Breast Cancer Res Treat 1992;21:3–13.
[3] Ferrans VJ. Overview of cardiac pathology in relation to anthracycline cardiotoxicity. Cancer Treat Rep 1978;62:955–61.
[4] Ferrans VJ. Anthracycline cardiotoxicity. Adv Exp Med Biol 1983; 161:519–32.
[5] Von Hoff DD, Rozencweig M, Layard M, Slavik M, Muggia FM. Daunomycin-induced cardiotoxicity in children and adults. A review of 110 cases. Am J Med 1977;62:200–8.
[6] Booser DJ, Hortobagyi GN. Anthracycline antibiotics in cancer therapy. Focus on drug resistance. Drugs 1994;47:223–58.
[7] Friche E, Skovsgaard T, Nissen NI. Anthracycline resistance. Acta Oncol 1989;28:877–81.
[8] Judson IR. Anthrapyrazoles: true successors to the anthracyclines? Anticancer Drugs 1991;2:223–31.
[9] Krapcho AP, Menta E, Oliva A, Di Domenico R, Fiocchi L, Maresch ME, Gallagher CE, Hacker MP, Beggiolin G, Giuliani FC, Pezzoni G, Spinelli S. Synthesis and antitumor evaluation of 2,5-disubstituted-indazolo[4,3-*gh*]isoquinolin-6(2*H*)-ones (9-aza-anthrapyrazoles). J Med Chem 1998;41:5429–44.
[10] Hazlehurst LA, Krapcho AP, Hacker MP. Comparison of aza-anthracenedione-induced DNA damage and cytotoxicity in experimental tumor cells. Biochem Pharmacol 1995;50:1087–94.
[11] Hazlehurst LA, Krapcho AP, Hacker MP. Correlation of DNA reactivity and cytotoxicity of a new class of anticancer agents: aza-anthracenediones. Cancer Lett 1995;91:115–24.
[12] Naito S, Yokomizo A, Koga H. Mechanisms of drug resistance in chemotherapy for urogenital carcinoma. Int J Urol 1999;6:427–39.
[13] Larsen AK, Escargueil AE, Skladanowski A. Resistance mechanisms associated with altered intracellular distribution of anticancer agents. Pharmacol Ther 2000;85:217–29.
[14] Ramachandra M, Ambudkar SV, Gottesman MM, Pastan I, Hrycyna CA. Functional characterization of a glycine 185-to-valine substitution in human P-glycoprotein by using a vaccinia-based transient expression system. Mol Biol Cell 1996;7:1485–98.
[15] Bolhuis H, van Veen HW, Poolman B, Driessen AJ, Konings WN. Mechanisms of multidrug transporters. FEMS Microbiol Rev 1997; 21:55–84.
[16] Stein WD. Kinetics of the multidrug transporter (P-glycoprotein) and its reversal. Physiol Rev 1997;77:545–90.
[17] Keizer HG, Schuurhuis GJ, Broxterman HJ, Lankelma J, Schoonen WG, van Rijn J, Pinedo HM, Joenje H. Correlation of multidrug resistance with decreased drug accumulation, altered subcellular drug distribution, and increased P-glycoprotein expression in cultured SW-1573 human lung tumor cells. Cancer Res 1989;49:2988–93.
[18] Engelke K, Krapcho AP, Hacker MP. The intracellular distribution of the 9-aza-anthrapyrazole compounds is regulated by the side chain terminal amines. Proc Am Assoc Cancer Res 1997;38:601.
[19] Hartley JA, Reszka K, Zuo ET, Wilson WD, Morgan AR, Lown JW. Characteristics of the interaction of anthrapyrazole anticancer agents with deoxyribonucleic acids: structural requirements for DNA binding, intercalation, and photosensitization. Mol Pharmacol 1988;33: 265–71.
[20] Sissi C, Moro S, Richter S, Gatto B, Menta E, Spinelli S, Krapcho AP, Zunino F, Palumbo M. DNA-interactive anticancer aza-anthrapyrazoles: biophysical, and biochemical studies relevant to the mechanism of action. Mol Pharmacol 2001;59:96–103.
[21] Safa AR. Photoaffinity labeling of the multidrug-resistance-related P-glycoprotein with photoactive analogues of verapamil. Proc Natl Acad Sci USA 1988;85:7187–91.
[22] Cornwell MM, Pastan I, Gottesman MM. Certain calcium channel blockers bind specifically to multidrug-resistant human KB carcinoma membrane vesicles and inhibit drug binding to P-glycoprotein. J Biol Chem 1987;262:2166–70.
[23] Altan N, Chen Y, Schindler M, Simon SM. Defective acidification in human breast tumor cells and implications for chemotherapy. J Exp Med 1998;187:1583–98.
[24] Marquardt D, Center MS. Drug transport mechanisms in HL60 cells isolated for resistance to doxorubicin: evidence for nuclear drug accumulation and redistribution in resistant cells. Cancer Res 1992; 52:3157–63.
[25] Patel DJ, Canuel LL. Anthracycline antitumor antibiotic·nucleic-acid interactions. Structural aspects of the daunomycin·poly(dA-dT) complex in solution. Eur J Biochem 1978;90:247–54.
[26] Patel DJ, Kozlowski SA, Rice JA. Hydrogen bonding, overlap geometry, and sequence specificity in anthracycline antitumor antibiotic·DNA complexes in solution. Proc Natl Acad Sci USA 1981;78:3333–7.
[27] Wang AH-J, Ughetto G, Quigley GJ, Rich A. Interactions between an anthracycline antibiotic and DNA: molecular structure of daunomycin complexed to d(CpGpTpApCpG) at 1.2-Å resolution. Biochemistry 1987;26:1152–63.
[28] Klohs WD, Steinkampf RW, Havlick MJ, Jackson RC. Resistance to anthrapyrazoles and anthracyclines in multidrug-resistant P388 murine leukemia cells: reversal by calcium blockers and calmodulin antagonists. Cancer Res 1986;46:4352–6.
[29] Lampidis TJ, Shi YF, Calderon CL, Kolonias D, Tapiero H, Savaraj N. Accumulation of simple organic cations correlates with differential cytotoxicity in multidrug-resistant and sensitive human and rodent cells. Leukemia 1997;11:1156–9.
[30] Lampidis TJ, Kolonias D, Podona T, Israel M, Safa AR, Lothstein L, Savaraj N, Tapiero H, Priebe W. Circumvention of P-GP MDR as a function of anthracycline lipophilicity and charge. Biochemistry 1997;36:2679–85.
[31] Friche E, Demant EJF, Sehested M, Nissen NI. Effect of anthracycline analogues on photolabelling of P-glycoprotein by [^{125}I]iodomycin and [^{3}H]azidopine: relation to lipophilicity and inhibition of daunorubicin transport in multidrug resistant cells. Br J Cancer 1993; 67:226–31.
[32] Molinari A, Cianfriglia M, Meschini S, Calcabrini A, Arancia G. P-glycoprotein expression in the Golgi apparatus of multidrug-resistant cells. Int J Cancer 1994;59:789–95.
[33] Belhoussine R, Morjani H, Sharonov S, Ploton D, Manfait M. Characterization of intracellular pH gradients in human multidrug-resistant tumor cells by means of scanning microspectrofluorometry and dual-emission-ratio probes. Int J Cancer 1999;81:81–9.
[34] Schindler M, Grabski S, Hoff E, Simon SM. Defective pH regulation of acidic compartments in human breast cancer cells (MCF-7) is normalized in adriamycin-resistant cells (MCF-7adr). Biochemistry 1996;35:2811–7.
[35] Raghunand N, Martínez-Zaguilán R, Wright SH, Gillies RJ. pH, and drug resistance. II, Turnover of acidic vesicles and resistance to weakly basic chemotherapeutic drugs. Biochem Pharmacol 1999;57: 1047–58.
[36] Martínez-Zaguilán R, Raghunand N, Lynch RM, Bellamy W, Martinez GM, Rojas B, Smith D, Dalton WS, Gillies RJ. pH, and drug resistance. I. Functional expression of plasmalemmal V-type H^+-ATPase in drug-resistant human breast carcinoma cell lines. Biochem Pharmacol 1999;57:1037–46.